Mathematical model for change in size distribution of baculovirus-infected Sf-9 insect cells

TAKESHI GOTOH*, MASAMICHI FUKUHARA, and KEN-ICHI KIKUCHI
Department of Materials-Process Engineering and Applied Chemistry for Environments
Akita University
1-1 Tegata Gakuen-Cho, Akita 010-8502
JAPAN
http://www.ipc.akita-u.ac.jp/~kankyo/

Abstract: - Sf-9 insect cells were examined for size before and after baculovirus infection. The distribution of the diameter of uninfected Sf-9 insect cells was described by the normal distribution function with the mean diameter and standard deviation of 18.5±1.5 μm. After virus infection, the cells grew in size almost linearly with time for about 48 h to give a steady mean diameter 1.45 times larger than that of uninfected cells. In addition, the distribution began to broaden at around 6 h-post infection and eventually had standard deviation twice as large as that of uninfected cells. A mathematical model was developed to simulate the size distribution of virus-infected Sf-9 insect cells at any given time after viral infection.

Key-Words: - Baculovirus, Sf-9, Insect cells, Size distribution, Mathematical model, Normal distribution

1 Introduction

The baculovirus expression vector system has been recognized as one of the most viable means for producing mammalian proteins not only in basic research field but also in the industrial production of vaccines and therapeutics, because of its ability to express a wide variety of proteins in high yield and of biological and immunological proper functionality of the produced proteins [1]. Several factors related to infection culture conditions have been revealed to significantly influence protein yields [2-6]. From an industrial perspective, these factors must be controlled properly so that the infection cultures yield a large amount of recombinant proteins. However, unexpected fluctuations sometimes occur in the course of the cultures probably due to diversity in cellular physiology and medium composition and inaccuracy in determining virus titer and cell density. Therefore, a certain index reflecting the physiological status of infected cells should be monitored during the cultures for proper operation.

It has been widely recognized that insect cells increase in size after baculovirus infection [7]. Since the cell enlargement can be determined without any laborious and/or costly pretreatments, it might be a good candidate to conveniently assess the status of virus infection [8]. However, information about the dynamics of cell size increase by virus infection has been limited. In the present study, Sf-9 insect cells are thoroughly examined for the trend of cell size distribution after baculovirus infection. A mathematical model is developed to simulate the change in cell size distribution.

2 Model for infected insect cell cultures

Model development for growth of insect cells, baculovirus infection, and progeny virus replication has been described elsewhere [9]. In brief, the virus infection of insect cells was described by the Poisson distribution function,

$$\Phi(t,j)=\frac{\exp\left\{-\alpha\left(V(t)/X_{\mathrm{U}}(t)\right)\right\}\left\{\alpha\left(V(t)/X_{\mathrm{U}}(t)\right)\right\}^{j}}{j!}, \quad (1)$$

where $X_{\mathrm{U}}(t)$ and $V(t)$ are the concentrations of viable uninfected cells and viruses at any given time t, respectively, and α is a proportionality constant that describes infection efficiency. The concentration of insect cells infected by at least one virus particle between t and (t+dt) were thus described by

$$n(t,\tau,j\neq 0)dt=1-\Phi(t,j=0)X_{\mathrm{U}}(t)\ , \quad (2)$$

where τ is a time after virus infection. The concentration of uninfected cells is increased according to the Monod expression (μ_{max}, K_S) and decreased by intrinsic cell death (k_D) and viral infection.

A cumulative Weibull distribution function was used to describe virus amplification by the infected cells, taking into account the effects of not only the number of viruses initially infecting the cells but also the inherent cellular activity on virus replication:

$$\Omega(\tau;\rho,\upsilon) = 1 - \exp\left\{-\left(\frac{\tau}{\upsilon}\right)^{\rho}\right\}, \quad (3)$$

where ρ is called a shape parameter to determine the shape of the distribution curves, υ is called a scale parameter for an index to the time of post-infection events such as progeny virus replication and infection-induced cell death. By using Eq(3), the change in virus concentration in a medium was described as follows:

$$\frac{dV(t)}{dt} = k_V \int_{\xi=0}^{\xi=\tau} f_{act} \left\{ \begin{array}{l} \Omega(\xi;\rho,\upsilon)\, n(t,\xi,j\neq 0) \\ -\Omega(\xi;\rho',\upsilon')\, n(t,\xi,j\neq 0) \end{array} \right\} d\xi - \sum_{j=1} j\, n(t,0,j), \quad (4)$$

where the first term represents the progeny virus replication and the second term accounts for the decrease by infection, and ξ is a temporal variable introduced for integration. Infected cells described by eq(2) begins to produce progeny viruses as characterized by the parameters ρ and υ and ceases the production due to the infection-induced cell death, which is also characterized by the parameters ρ' and υ'. k_V is an intrinsic specific virus replication rate. Since the virus replication was known to be largely influenced by the infecting cell density (ICD) that is defined as the cell density at time of infection, an ICD-dependent correlation factor f_{act} was introduced.

3 Experimental

3.1 Cell and virus

The insect cell line, *Spodoptera frugiperda* (Sf-9), was grown in suspension cultures at 28°C in serum-free SF-900 II medium (Invitrogen, Carlsbad, CA, USA). A recombinant strain (vGFPuv) of *Autographa californica* nuclear polyhedrosis virus was used as a baculovirus, containing a gene encoding a variant of green fluorescent protein fused into the polyhedrin gene which is under the control of a polyhedrin promoter [10]. The virus was titered for plaque forming units (pfu) per ml by the end point dilution assay [11].

3.2 Infection

Sf-9 insect cells at the mid-exponential growth phase were used for baculovirus infection. For synchronous infection, Sf-9 cells harvested by centrifugation were resuspended in a fresh medium at a density of 1 x 10^7 cells ml^{-1} and infected with vGFPuv by the addition of a virus stock at a high MOI of 20 pfu $cells^{-1}$. After incubation for 1 h, the cells were diluted with a fresh medium to give a density of 1 x 10^6 cells ml^{-1} and then cultured at 28°C at 100 rpm. For unsynchronous infection, Sf-9 cells were infected at 3 x 10^6 cells ml^{-1} at an appropriate MOI and then cultured in the same way as described above.

3.3 Analysis of cell size

Uninfected and virus-infected Sf-9 insect cells were observed under an optical microscope equipped with a digital camera. The digitized images of at least 1000 cells were analyzed for cell size distribution using image analysis software (ARGUS-50, Hamamatsu Photonics, Sizuoka, Japan).

4 Results and Discussion

4.1 Size distribution of uninfected Sf-9 cells

The microscopic digitized 2D images of Sf-9 insect cells were taken and analyzed for cell diameter. Fig. 1A shows a typical example of frequency distribution (histogram) in a small increment of diameter determined for uninfected Sf-9 cells, giving the mean cell diameter and standard deviation of 18.5±1.5 μm. The histogram is well agreed with a curved flaring shape shown by the normal distribution function,

$$F(d;\bar{d},\sigma) = \frac{1}{\sigma\sqrt{2\pi}} \exp\left\{-(d-\bar{d})^2 / 2\sigma^2\right\}, \quad (5)$$

where $\bar{d}$ and σ are mean cell diameter and standard deviation, respectively. This indicates that the uninfected Sf-9 insect cells are normally distributed in size.

4.2 Size distribution of infected Sf-9 cells

4.2.1 Synchronous infection

To analyze the trend in the diameter change of virus-infected Sf-9 insect cells, the virus infection was carried out as synchronously as possible. Fig. 1B

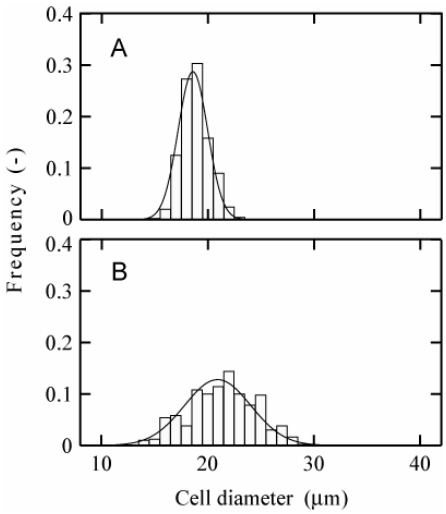

Fig. 1 Size distribution of Sf-9 insect cells. A, uninfected Sf-9 cells; B, virus-infected Sf-9 cells at 24 h-hvi, which were infected at a MOI of 20 pfu cells^{-1}. Bars, experiment; curves, calculations by the normal distribution function.

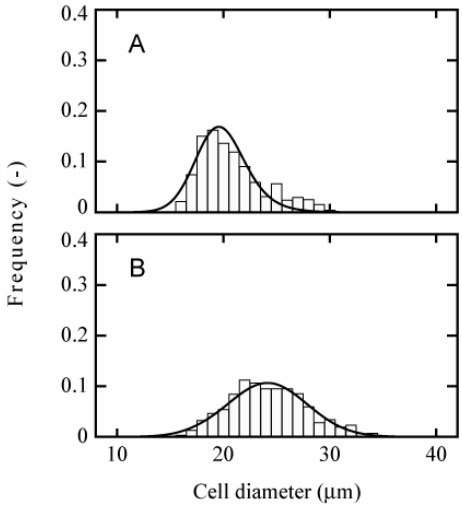

Fig. 3 Size distribution of unsynchronously infected Sf-9 insect cells (MOI=0.5 pfu cells^{-1}) at (A) 24 and (B) 48 h-pvi. Bars, experiments; Curves, model calculations.

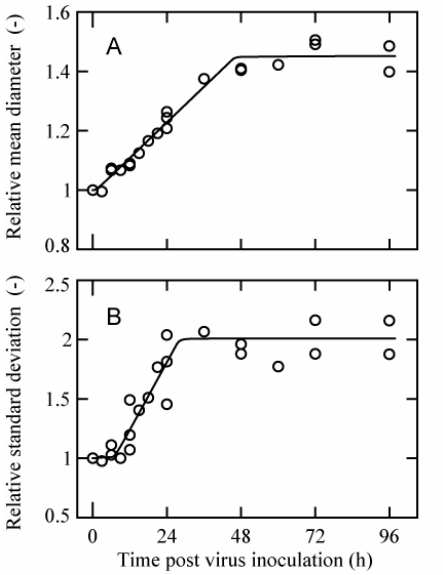

Fig. 2 Sequential changes in mean diameter and standard deviation of virus-infected Sf-9 insect cells. Curves are calculations by the model developed in the present study.

shows the cell diameter frequency distribution of virus-infected Sf-9 cells at 24 h-post virus inoculation (pvi). The distribution is apparently shifted to the larger side and broadened, compare to that of uninfected cells. The resemblance of shapes between the distribution and calculation curve indicates that the synchronously infected Sf-9 cells are also normally distributed in size.

Sequential change in the mean diameter and standard deviation of the synchronously infected Sf-9 cells were determined (Fig. 2). After the virus inoculation the mean cell diameter apparently increases almost linearly by 2 d-pvi to reach a maximum value, which is 1.45 times as large as that of uninfected cells. The standard deviation, meanwhile, has a lag period of about 6 h, after which linearly increases to be a steady value of double.

4.2.2 Unsynchronous infection

In low MOI infection cultures, the primary infection by the initially inoculated viruses occurs within a limited short period of time. Uninfected cells continue to grow until the cells are secondarily infected by progeny viruses budded from the primary infected cells. This unsynchronous infection process is expected to affect the cell size distribution. Fig. 3 depicts the cell diameter frequency distribution of unsynchronously infected Sf-9 cells (MOI=0.5 pfu cell^{-1}). The diameter distribution of the culture is not significantly shifted yet at 24 h-pvi, but a small tailing is observed at the larger side of the distribution; this seems due to a primary infection. At 48 h-pvi the distribution was broadened and collectively shifted toward the larger side like the synchronous (high MOI) infection cultures.

4.3 Model development for cell size distribution

A cell subset generated immediately after virus infection between t and (t+dt) according to the Poisson distribution equation is normally distributed in size and expected to change the distribution with τ as observed in Fig. 2. To describe the increase in diameter and the broadening in size distribution of the infected cells, we suppose that the mean diameter and standard deviation for individual infected cell subsets increase according to partial linear relationships with respect to τ as follows:

$$r_d(\tau)=\frac{\bar{d}(\tau)}{\bar{d}_{\mathrm{U}}}=\begin{cases}\dfrac{1.45\tau}{\tau_{\mathrm{d}}}+1 & (0\le\tau<\tau_{\mathrm{d}})\\ 1.45 & (\tau\ge\tau_{\mathrm{d}})\end{cases}, \tag{6}$$

$$r_\sigma(\tau)=\frac{\sigma(\tau)}{\sigma_{\mathrm{U}}}=\begin{cases}1.0 & (0\le\tau<\tau_{\sigma\mathrm{L}})\\ \dfrac{\tau-\tau_{\sigma\mathrm{E}}}{\tau_{\sigma\mathrm{L}}-\tau_{\sigma\mathrm{E}}}+1 & (\tau_{\sigma\mathrm{E}}\le\tau<\tau_{\sigma\mathrm{L}})\\ 2.0 & (\tau\ge\tau_{\sigma\mathrm{L}})\end{cases}, \tag{7}$$

where $\bar{d}_{\mathrm{U}}$ and σ_{U} are the mean diameter and standard deviation of uninfected cells, respectively. The overall apparent size frequency distribution at any given time is obtained by dividing the sum of the frequency distributions of all the virus-infected cell subsets and uninfected cells by the total cell concentration $X_{\mathrm{T}}(t)$ as follows:

$$F_{app}(d)=\frac{1}{X_{\mathrm{T}}(t)}\Big\{F(d;\bar{d}_{\mathrm{U}},\sigma_{\mathrm{U}})X_{\mathrm{U}}(t)+\int_{\xi=0}^{\xi=\tau}F\big(d;\bar{d}(\xi),\sigma(\xi)\big)n(t,\xi,j\ne0)d\xi\Big\}. \tag{8}$$

4.4 Model calculation of size distribution of infected Sf-9 cells

All the parameters used for the calculations of size distribution of virus-infected Sf-9 insect cells were listed in Table 1. The parameters concerned with virus infection cultures of Sf-9 insect cells were obtained from the literature. The time parameters, τ_{d}, $\tau_{\sigma\mathrm{E}}$, $\tau_{\sigma\mathrm{L}}$, responsible for the change in cell size distribution were determined so that the calculation best fitted the experimental results. The calculations are also shown in Fig. 2.

The cell size distribution was calculated by the model for various virus-infected Sf-9 insect cell cultures. As shown in Fig. 3, the low MOI infection culture, having a small tailing in the larger region of the size distribution at 24 h-pvi, is relatively well simulated as a sum of virus-infected and uninfected cells, both of which coexist at the early time post virus inoculation. The model also simulates the subsequent broadening of the distribution, which is indistinguishable from that for a high MOI infection cultures at 48 h-pvi.

Table 1 Parameters used in the model calculation.

Parameter	Value	Unit	Reference
μ_{max}	0.04	h^{-1}	[4], [9]
K_S (for L-glu)	2.5	mM	[9]
k_D	0.0008	h^{-1}	[12]
α (at high cell den.)	0.16	-	This paper
(at mid cell den.)	0.08	-	[13]
τ_d	45	h	This paper
$\tau_{\sigma E}$	6	h	This paper
$\tau_{\sigma L}$	24	h	This paper
X_{High}	5.1 x10^6	cells ml^{-1}	[9]
X_{Low}	1.3x10^6	cells ml^{-1}	[9]
k_V	20	pfu $cell^{-1}$ h^{-1}	[13]
ρ, ρ'	3	-	[9]
σ	18	h	[9]
σ'	75	h	[9]

Fig. 4 compares the cell size distribution of various MOIs infection cultures at 24 h-pvi. The higher MOI the cells are infected, the larger size region the cells are distributed. On the whole, this tendency is well demonstrated by the calculation.

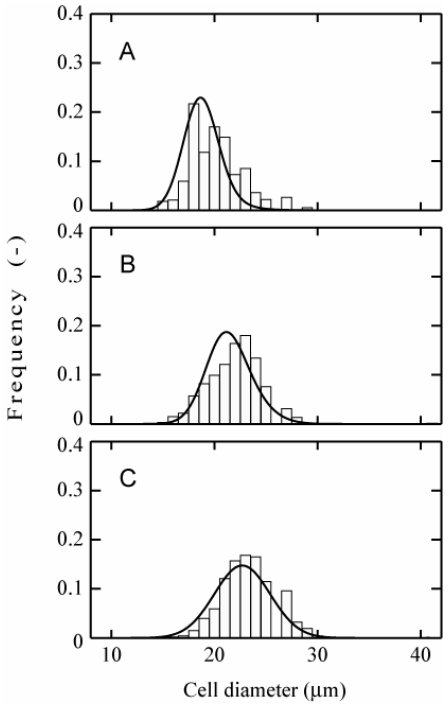

Fig. 4 Size distribution of Sf-9 insect cells infected at various MOIs at 24 h-pvi. MOI: A, 0.1 pfu $cells^{-1}$; B, 1 pfu $cells^{-1}$; C, 10 pfu $cells^{-1}$. Bars, experiments; curves, model calculations.

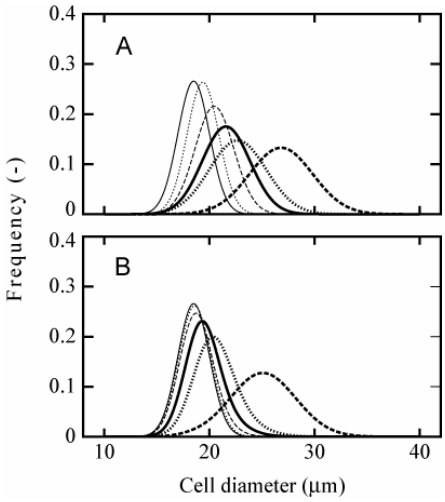

Fig. 5 Model simulation of chronological transition of size distribution of virus-infected Sf-9 insect cells. A, MOI=10 pfu cells^{-1}; B, MOI=0.5 pfu cells^{-1}. Curves: ——, 0 h-pvi; ·····, 6 h-pvi; - - - -, 12 h-pvi; ——, 18 h-pvi; ·····, 24 h-pvi; – – –, 48 h-pvi.

The chronological transition of the size distribution of Sf-9 insect cells was calculated for high and low MOI infection cultures (Fig. 5). The distribution is shifted toward a larger size with increasing time, and the shift for a high MOI culture is faster than that for a low MOI culture, especially until 24 h-pvi. At 48 h-pvi, however, the difference in the distribution between the two infection cultures was insignificant.

5 Conclusion

The cell size distribution of virus-infected Sf-9 insect cells was examined and a mathematical model was developed to describe the sequential change in the distribution. The model calculation simulated the trend of size distribution of Sf-9 insect cells infected under various conditions. Since the cell size distribution analysis does not require any laborious tasks or expensive reagents, the model calculation would give a simple and convenient chart to assess the degree of virus infection.

References:

[1] Luckow, V. A. Protein production and processing from baculovirus expression vectors. *In* Baculovirus expression systems and biopesticides; Shuler, M. L., Wood, H. A., Granados, R. R., Hammer, H. A., Eds.; Wiley-Liss: New York, 1995, pp. 51-90.

[2] Licari, P, Bailey, J. E. Factors influencing recombinant protein yields in an insect cell-baculovirus expression system: multiplicity of infection and intracellular protein degradation. *Biotechnol. Bioeng.*, 1991, 37, pp. 238-246.

[3] Kioukia, N., Nienow, A. W., Emery, A. N., Al-Rubeai, M. Physiological and environmental factors affecting the growth of insect cells and infection with baculovirus, *J. Biotechnol.*, 1995, 38, pp. 243-251.

[4] Taticek, R. A., Shuler, M. L. Effects of elevated oxygen and glutamine levels on foreign protein production at high cell densities using the insect cell-baculovirus expression system. *Biotechnol. Bioeng.*, 1997, 54, pp. 142-152.

[5] Gotoh, T., Miyazaki, Y., Chiba, K., Kikuchi, K.-I., Significant increase in recombinant protein production of a virus-infected Sf-9 insect cell culture of low MOI under low dissolved oxygen conditions. *J. Biosci. Bioeng.*, 2002, 94, pp. 426-433.

[6] Gotoh, T., Chiba, K., Kikuchi, K.-I. Oxygen consumption profiles of Sf-9 insect cells and their culture at low temperature to circumvent oxygen starvation. *Biochem. Eng. J.*, 2004, 17, pp. 71-78.

[7] Nordström, T., Willamo, M., Arvela, M., Stenroos, K., and Lindqvist, C. Detection of baculovirus-infected insect cells by flow cytometric side-scatter analyses. *Cytometry*, 1999, 37, pp. 238-242.

[8] Palomares, L. A., Pedroza, J. C., and Ramirez, O.T., Cell size as a tool to predict the production of recombinant protein by the insect-cell baculovirus expression system, *Biotechnol. Lett.*, 2001, 23, pp. 359-364.

[9] Gotoh, T., Chiba, K., Kikuchi, K.-I., Probabilistic characterization for baculovirus- infected insect cells destined to produce progeny viruses and recombinant protein and to die. *J. Chem. Eng. Jpn*, 2004, 37, pp. 1357-1366.

[10] Cha, H. J., Gotoh, T., Bentley, W. E., Simplification of titer determination for recombinant baculovirus by green fluorescent protein marker. *BioTechniques*, 1997, 23, pp. 782-786.

[11] O'Reilly, D. R., Miller, L. K., Luckow, V. A., Baculovirus expression vectors: a laboratory manual. Freeman: New York, 1992.

[12] Dalal, N. G., Bentley, W. E., Mathematical characterization of insect cell (Sf-9) death in suspended culture. *Biotechnol. Lett.*, 1999, 21, pp. 325-329.

[13] Hu, Y.-C., Bentley, W. E., A kinetic and statistical thermodynamic model for baculovirus infection and virus-like particle assembly in suspended insect cells. *Chem. Eng. Sci.*, 2000, 55, pp. 3991-4008.